DMIC

JPRS: 25,054

OTS: 64-31467

11 June 1964

064431

ARC-DISCHARGE METALLURGY

- USSR -

U. S. DEPARTMENT OF COMMERCE
OFFICE OF TECHNICAL SERVICES
U. S. JOINT PUBLICATIONS RESEARCH SERVICE
Building T-30
Ohio Drive and Independence Avenue, S.W.
Washington 25, D. C.

Price: $1.50

FOREWORD

This publication was prepared under contract for the Joint Publications Research Service as a translation or foreign-language research service to the various federal government departments.

The contents of this material in no way represent the policies, views or attitudes of the U. S. Government or of the parties to any distribution arrangement.

PROCUREMENT OF JPRS REPORTS

All JPRS reports may be ordered from the Office of Technical Services. Reports published prior to 1 February 1963 can be provided, for the most part, only in photocopy (xerox). Those published after 1 February 1963 will be provided in printed form.

Details on special subscription arrangements for any JPRS report will be provided upon request.

No cumulative subject index or catalog of all JPRS reports has been compiled.

All current JPRS reports are listed in the Monthly Catalog of U. S. Government Publications, available on subscription at $4.50 per year ($6.00 foreign), including an annual index, from the Superintendent of Documents, U. S. Government Printing Office, Washington 25, D. C.

All current JPRS scientific and technical reports are cataloged and subject-indexed in Technical Translations, published semimonthly by the Office of Technical Services, and also available on subscription ($12.00 per year domestic, $16.00 foreign) from the Superintendent of Documents. Semiannual indexes to Technical Translations are available at additional cost.

JPRS: 25,054

ARC-DISCHARGE METALLURGY

- USSR -

Following is a translation of five articles in the Russian-language book Elektroiskrovaya Obrabotka Metallov (Electrical Discharge Treatment of Metals), Academy of Sciences Publishing House, Moscow, 1963. Complete bibliographic information accompanies each article.

TABLE OF CONTENTS

A STUDY OF CRYSTAL STRUCTURE DEFECTS IN PURE METALS DURING SPARK DISCHARGE

[Following is a translation of an article by L. C. Palatnik, A. A. Levchenko and V. M. Kosevich appearing in the Russian-language book Elektroiskrovaya Obrabotka Metallov (Electrical Discharge Treatment of Metals), Academy of Sciences Publishing House, Moscow, 1963, pages 104-112.]

The influence of electrical discharge on electrodes results in extremely rapid heating and cooling of the metal in local areas of the surface layer [1]. This creates favorable conditions for the arising of various kinds of defects in the crystal structure in the zone of influence of the discharge. An investigation of crystal structure defects appearing under the influence of spark discharges represents interest from the viewpoint of the stucy of the mechanism of electrical erosion of metals, physico-chemical shanges in surface layers, mechanical surface properties, etc.

In this work, we will investigate the formation of sych imperfections in crystal structure as dislocations, packing defects, vacancies.

Dislocation defects were revealed in single crystals of bismuth, antimony and zinc by selective etching. Vacancies and packing defects were revealed by X-ray methods in polycrystalline samples of pure metals -- gold, silver and copper.

An Investigation of the Distribution of Dislocation Defects Appearing in Single Crystals Under the Action of Spark Discharges

As sources for spark discharges, we used an IG-2 generator, used in spectral analysis and an electrospark intensifier (constructed by Kharkov Technical Plant). The results achieved by exposing crystals to sparks from the two generators coincided qualitatively. However, the behaviour of individual traces of the sparks is clearer with the IG-2 generator. Therefore, the illustrative material below was all obtained

using the IG-2 generator.

The surface of samples exposed to sparks and etched showed chipping of single srystals along cleavage plane (111) for bismuth and antimony and (001) for zinc. The samples were etched in the following solutions in order to reveal the dislocation defects: for bismuth -- 20% conc. HNO_3 in glacial acetic acid; for zinc -- 7% fuming HCl in glacial acetic acid; for antimony -- etching agent type SR-4 [2].

Each sample was submitted to preliminary etching. Then the surface of the sample with the least number of dislocations was subjected to the action of the discharge, and the crystal was etched a second time. The second etching revealed a large number of new etching pits near the anode and cathode traces of the discharge, indicating the intense formation of new dislocations.

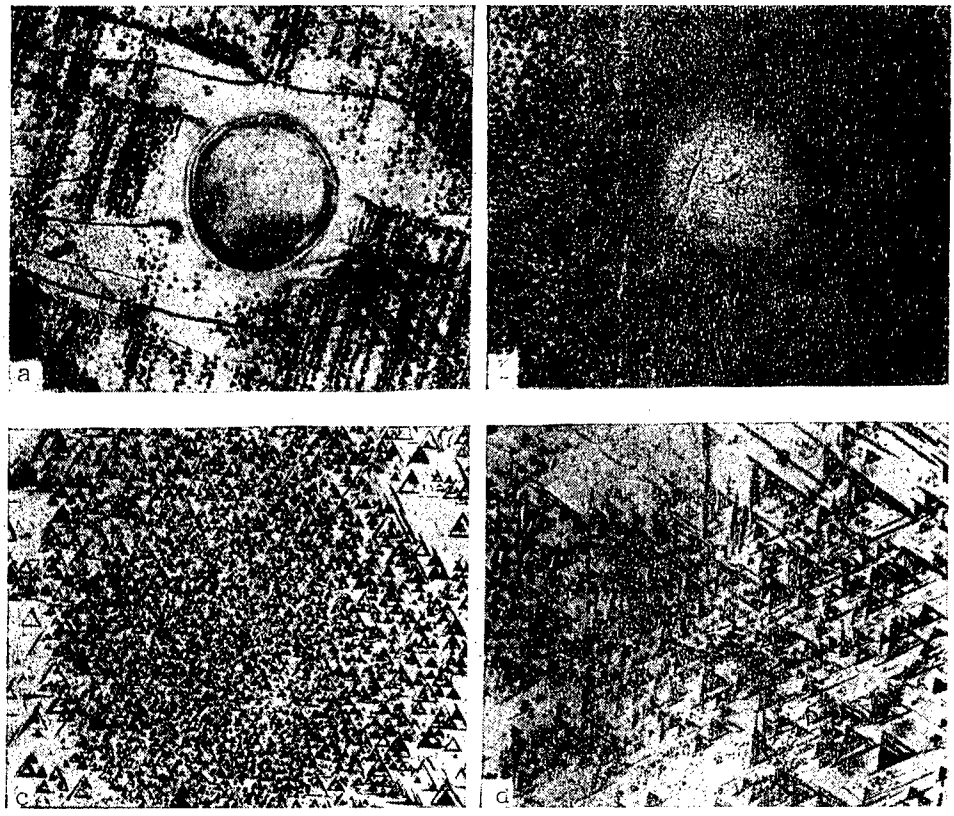

Figure 1
Photomicrography of pits formed during etching of bismuth; a -- anode hole in etched surface (111); b -- additional etching in the same place; c -- etching to a depth of 50 microns; d -- etching to a depth of 100 microns.

Figure 1a shows the plane of cleavage of cleavage of bismuth after etching in the initial state, figure 1b shows the same section after additional etching of the region of an anode trace [see note]. As can be seen from figure 1b, the new dislocations near the anode hole are concentrated in a zone of limited area. The diameter of this zone ex-

ceeds the diameter of the anode hole considerably, by a factor of four or five.

[note]: editor's note: the terms "anode trace" and "cathode trace" as used by the authors of this article cannot be taken strictly, since during experimentation they used both the high frequency IG-2 spark generator and the Kharkov model electrospark apparatus, which does not produce aperiodic (unipolar) discharges. Furthermore, the results of spark treatment with the IG-2 cannot fully illustrate the picture of what will happen with single spark discharge treatment.

The etching agent used on the bismuth crystals was also used to illustrate the degree of diclocation at various depths below the surface by consecutive etching of layers of the sample. This method determined the volume picture of the distribution of dislocations in sections of a crystal exposed to spark discharge.

As an example, on figure 1c and 1d are shown the results of spark discharge treatment at depths of 50 and 100 microns.

The etching method revealed both the qualitative and quantitative aspects of the distribution of dislocations. Figure 2 shows the quantitative distribution of dislocation defect densities (,cm^{-2}) in the region of an anode trace on bismuth against the distance from the center of the trace. Naturally, the density of dislocations was highest at the center of the hole, and decreased with increasing distance from it. The density of dislocations at the maximum was $2 \cdot 10^7$ cm^{-2}, which exceeded the maximum density of dislocations in the initial crystal by two orders of magnitude. Curve I (fig. 2) shows the distribution of dislocation defects on the surface of the sample, the other curves show the distributions at various depths below the surface.

The graph in figure 2 shows that the zone filled with the new dislocations has rather sharp borders at all depths. This allowed construction of its profile in planes passing through the center of the hole and perpendicular to the plane of spark treatment (see solid line on fig. 3). The dotted lines on figure 3 show the regions with varying degrees of dislocation density.

The volume picture of the distribution of cislocations, shown in figure 3, indicates that the most intense formation of dislocations during spark treatment occured in the thin surface layer. Here the density of dislocations was 10^7 cm^{-2}, whereas the main volume of the affected zone contained dislocations with a density of $5 \cdot 10^5$ -- $1 \cdot 10^6$ cm^{-2}. It should be noted that the depth of the zone containing new dislocations exceeded the depth of the anode trace by 10-20 times.

The distribution of dislocations near the cathode trace was significantly different from the distribution near the anode traces

(figure 4a,b). In the first place, the diameter of the zone of dislocations exceeded the diameter of the cathode trace by only 2-3 times. Second, near the cathode hole, the etching pits were displaced in two rings: the inner, dark ring and the outer, lighter ring. In figure 4b, this can be clearly seen. At great magnifications it could be seen that the dark ring consisted of deep, sharp edged pits, and the light ring of smaller, shallow, flat-bottomed pits. The flat-bottomed pits appear usually in places where shallow dislocation loops are etched. Therefore the light external ring should be considered as the location of the dislocations in the thin surface layer of the crystal.

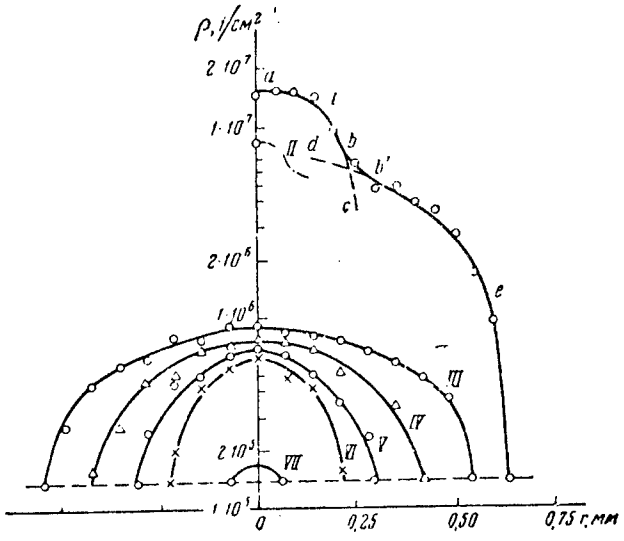

Figure 2

Distribution of dislocation plane ϱ near the anode trace in bismuth (zero of coordinate r corresponds to center of hole): I -- at the surface, II -- at 12.5 microns, III -- 25 microns, IV -- 50 microns, V -- 75 microns, VI -- 100 microns, VII -- 125 microns.

The graph of dislocation density distribution near the cathode hole in bismuth (figure 5) clearly shows the separation of the zone of dislocations into the two parts (branches klm and nl'p). Layer-by-layer etching of a bismuth crystal containing a cathode hole showed that the density of cislocations was sharply reduced at a depth on the order of 25 microns.

Figure 6 shows the picture of etching of an anode trace in plane (001) of a zinc monocrystal. The diameter of the zone of new dislocations exceeded the diameter of the trace by a factor of 3-5 (for the cathode trace in zinc this ratio of diameters was only 1.3-1.7).

The main characteristic of the distribution of dislocations near individual traces in zinc was the fact that the new dislocations were concentrated in a zone bounded by a hexagon, whose sides were parallel to the directions of prismatic slipping /10-12/.

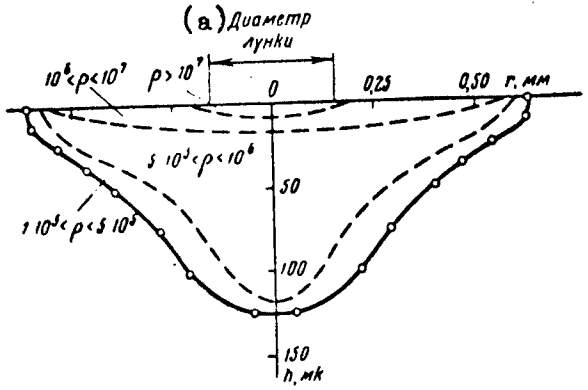

Figure 3.
Profile of the zone containing new dislocations near the anode hole. Key: a, hole diameter.

We also investigated the effect of repeated spark discharges on the formation of dislocation defects in crystals of bismuth, antimony and zinc. Figure 7 shows a perpendicular section of a spark discharge zone on a bismuth monocrystal. Attention was attracted by the fact that multiple spark treatment formed a large quantity of macroscopic defects -- pores with diameters of 1--5 microns. The pores in fig. 7 look like black points, but with magnification by 1,000 diameters, they reveal crystalline faceting with type (100) planes.

Let us discuss the experimental data obtained.

The formation of dislocations during electrospark treatment of crystals can occur, in our opinion, as a result of the physical processes of: point hardening [1] by rapid cooling from liquid to crystalline state [see note]; the formation of a pulse field of thermal stresses; disruption of the surface of the air shock wave, appearing in the interelectrode gap [3].

[note]: ed. note: the term "hardening" here is not quite proper, since after the moment of crystallization, sharp cooling in the given case could also not lead to the formation of metastable structures.

In connection with this, the total distribution of dislocations

in the spark destruction zone can be divided into individual areas, each of which corresponds to one of the various physical prodesses which cause the formation of dislocations.

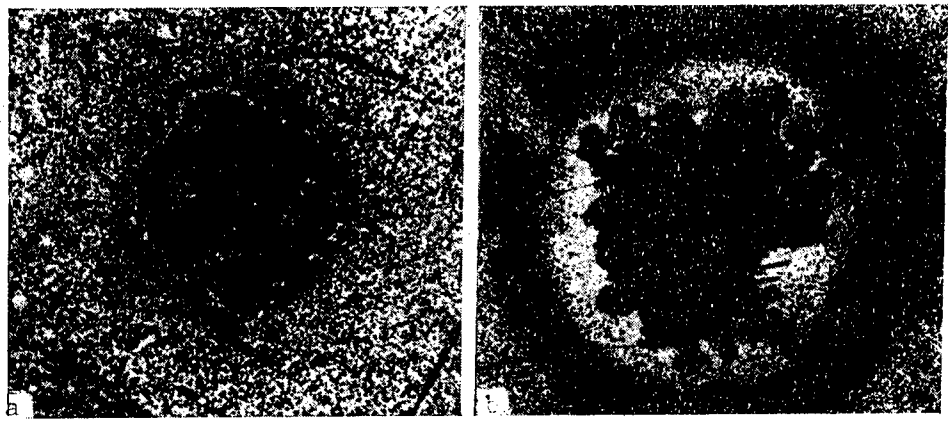

Figure 4.
Cathode trace after repeated etching: a -- in plane (111) of bismuth (X 70); b -- in plane (111) of antimony (X 135).

The air shock wave can lead to the formation of dislocations only in the thin surface layer. Apparently it is the cause of the areas of small dislocation loops which are especially clearly seen near the cathode holes in antimony crystals (figure 4b). Curves describing the distribution of dislocations near the cathode traces (figure 5) divide into two branches klm and nl'p. It can be supposed that the branch nl'p describes the distribution of dislocations which appear under the influence of the shock wave in the air.

Point hardening, connected with melting of the crystal, is characteristic for the anode discharge. The distribution of dislocations appearing as a result of melting and rapid crystallization is described by branch abc of curve I, figure 2. It is characteristic that distribution graphs at a certain depth from the anode trace (for example curve II, fig. 2) no longer show points of inflection. Consequently, at the corresponding depth from the surface, the crystal is not melted.

The greatest volume of metal in the zone of spark destruction is occupied by the dislocations arising under the influence of thermal

stresses. The distribution of these dislocations near each hole (fig. 5) is characterized by branch klm near the anode hole (fig. 2) -- branch db'l of curve I and curves III -- VII throughout their entire lengths.

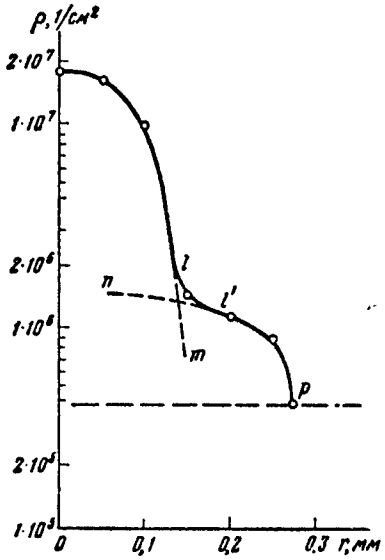

Figure 5
Distribution of dislocation density ϱ near cathode trace.
Zero of coordinate r is located at the edge of the trace.

Dislocations caused by thermal stresses occupy a much greater area near the anode trace that near the cathode trace. This can be explained by the fact that the formation of a stable dislocation loop requires a certain finite time interval.

If the duration of the thermal stress impulse is less than this interval, no dislocations will arise. It has been established [4] that the process of electrical erosion at the cathode is carried out by a micro-explosion. Thermal stresses at the cathode arise so fast that the breaking stress is achieved and particles of metal are separated before there is time for a noticeable number of dislocations to form. At the anode, the process of electrical erosion takes place by melting of the metal, and the thermal stress wave is of longer duration. Naturally, in this case the zone of dislocations is larger, a fact which has been experimentally observed.

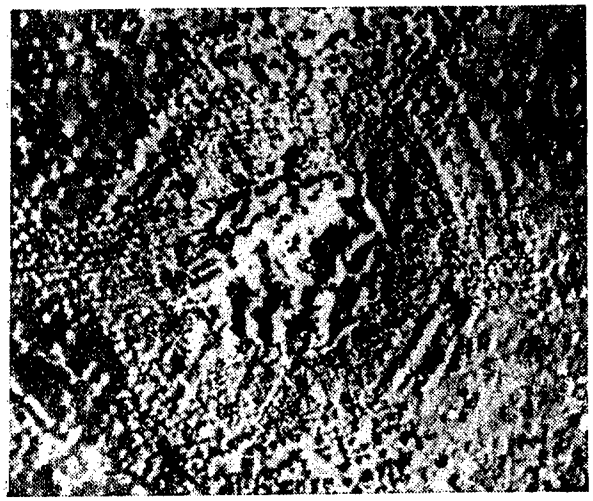

Figure 6. Etching near anode trace on plane (0001) in zinc (X 70).

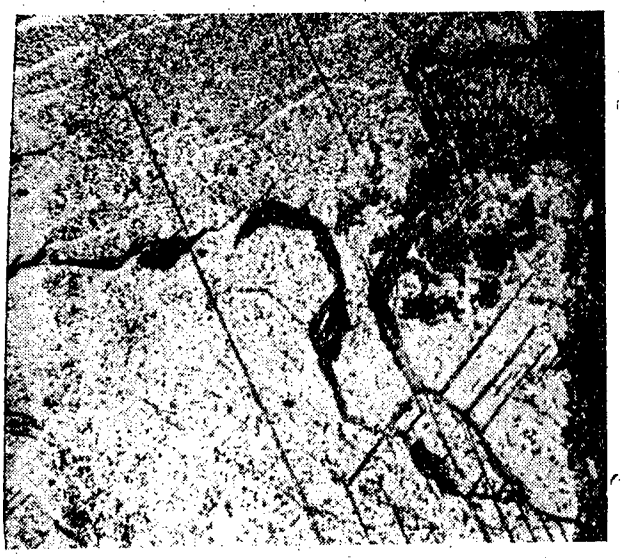

Figure 7. Etching of zone of treatment by repeated fluctuating discharges (perpendicular section of zone damaged by discharges, x 70).

A study of the Formation of Vacancies and Packing Defects Under the Influence of Spark Discharges

As subjects for investigation in this part of the work we used polycrystallic samples of copper, gold and silver of not less than 99.99% purity. The samples were subjected in the initial state to control X-ray exposure, which revealed that the parameters of the lattices of the initial metals corresponded with the values in the literature with accuracy of up to 0.01% (see table).

Spark processing of the samples was done with an IG-2 generator with the following operating conditions: inductance L=0, current strength I=3a, capacitance C= 0.02 mf, spark exposure time -- from 3 to 60 sec.

In order to determine the changes in parameters of the crystal lattice of the samples exposed to spark action, Sachsograms were made under cobalt radiation with the following screens: silver, for the gold and copper samples; and iron for the silver samples. The calculations were performed according to the line (420): error in determination of the period of the lattice did not exceed 0.01 --0.02%.

The measurement of lattice parameters for a large number of samples of gold, silver and copper invariably indicated the lessening of parameter a after exposure to the spark. From the table, in which the most characteristic results are shown, it can be seen that parameter a in gold decreases by 0.095%, in silver by 0.07%, in copper by 0.085%.

A decrease in the parameter of the crystal lattice of a pure metal can be caused by the following factors: the hardening of vacancies; the formation of a solid solution of substitution with an element with a smaller atomic diameter than the element under investigation; the formation of first order stress.

Values of the Parameter a of the Crystal Lattice of Copper, Gold and Silver in Various States

Metal	Copper	Gold	Silver
Literature value, kX /5/.	3.6080	4.0704	4.0779
Initial samples, kX.	3.6087	4.0701	4.0777
After exposure, kX	3.6054	4.0662	4.0750
Decrease in parameter, $\frac{\Delta a}{a}$ %	-0.085	-0.095	-0.07

The formation of solid substitution solutions was excluded in our case for the following reasons. Both electrodes in our experiments were of the same metal , so that a solid "metal-metal" solution could not be

formed. The assumption of the solution of gasses is unsuitable, since none of them results in solid substitution solutions with the metal, and the formation of all known solid solutions of penetration leads to an increase in the crystal lattice parameter.

Special X-ray investigations using slanting exposures also showed the abscence of significant first order stresses in the investigated layer. In connection with this, it must be considered that the observed decrease in the parameter of the crystal lattice is caused by the hardening of vacancies and the formation of packing defects.

We will estimate first of all the concentration of "hardened" vacancies which would cause the experimentally observed decrease in lattice parameter. In an approximation of Vegard's rule and in the assumption that the volume of a vacancy is equal to zero, the concentration $C = \frac{\Delta a}{a} \cdot 100\%$, where Δa is the difference in parameters in the initial and spark-treated samples. Calculation gives: for copper, C= 0.85%, for gold, C= 0.095% and for silver, C= 0.07%. However, these figures are low. According to the latest theoretical investigations /6/ the volume occupied by a vacancy is not equal to zero, but rather is 0.32 -- 0.44 of the atomic volume. In this case, the concentration of vacancies can be evaluated by the formula:

$$C = \frac{\Delta a}{a - \sqrt[3]{0{,}44a}} 100\%.$$

Calculation by this formula gives an even higher concentration of vacancies: for copper, 0.38%; for silver, 0.29%, and for gold, 0.40%. Further, it should be noted that the usage of various lines on the roentgenogram for the calculation for the parameter of the lattice of an exposed metal leads to the accumulation of varying data for the value of the parameter (fig. 8), where the values of a, calculated for lines (420) and (331) are shown. The parameter found using line (331) is lower than that found using line (420). The difference in the values of the parameter exceeded the maximal error in the experiment by a factor of 3 -- 5, and therefore could not be attributed to chance factors.

As was noted, an even greater quantity of dislocations arose in the process of spark treatment of monocrystals. Under the same conditions which favor the formation of dislocations, the formation of defects in crystal structure of a somewhat different type also usually occurs, that of the so called packing defects, which are a disruption of the order of placement of the atomic layers. Packing defects arise most easily in metals for which the energy for formation of packing defects

is rather low. Such metals include the metals which we investigated: gold (γ=33 erg/cm^2), silver (γ=35 erg/cm^2), copper (γ=50 erg/cm^2).

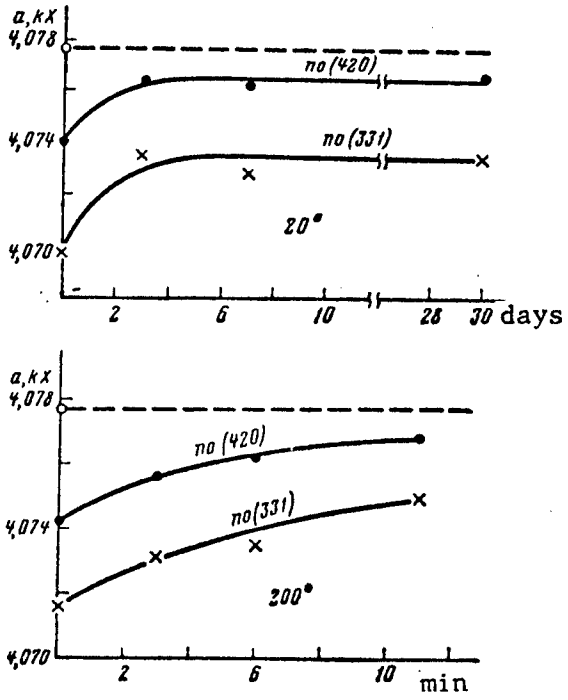

Figure 8.
Change of parameter a of the crystal lattice of spark-treated silver during retention at various temperatures (a initially = 4.0777).

Changes in the intersurface distance in the crystal are the only effects of packing defects. For example, the distance between (331) surfaces in the crystal decreases. Therefore, calculation of the lattice parameter according to the (331) lines yields a lowered value for a (fig. 8). It is natural to treat the observed difference in the values of parameter a obtained with various lines as the result of packing defects. Using a formula from work /7/ for calculation, we obtain a packing defect concentration of 1%. This means that of every 100 atomic planes, one plane has improper packing of the atoms.

The imperfections of crystal structure which arose during spark treatment of the metals turned out to be thermally unstable. This can be seen from the fact that in the process of heating or even storage at room temperature, the parameter of the crystalline lattice of spark-treated metal tends to return to its initial value. In figure 8a are seen graphs of the change in parameter a of a silver lattice in the process of retention at room temperature. The data are shown as

calculated for lines (420) and (331). The retu n of the parameter to its initial value can be accelerated by heating the sample. In fig. 8,b are shown graphs of the change in parameter a with time at various temperatures. As can be seen from the graph, at a temperature of 300° parameter a returms to the initial valur in only 6 minutes.

The results of heating of crystal samples additionally indicated that the reason for the decrease in the parameter during spark treatment was vacancies. It is a known fact that excess vacancies have rather high mobility, easily migrate to the surface, settle in micropores, dislocations, accumulate in colonies which are the cause of the formation of dislocation loops. A large number of dislocation defects, like that in the zone of action of the discharge, create favorable conditions for the drain of vacancies. The complete return of the parameter to initial value in only 6 minutes at 300° fully agrees with the assumptions made concerning the annealing of crystal vacancies.

In the experiments on the annealing of spark-treated samples can be found confirmation also of the fact that imperfections in the crystal structure of the packing defect type arise. It is obvious that packing defects have greater thermal stability than vacancies, therefore higher temperatures are necessary to heal them, as well as longer annealing times. These very conclusions follow from an analysis of the kinetics of annealing by interference lines (420) and (331) (figure 8a,b,c). It can be seen from fig. 8,a that the difference in apparent values $a=a_{420}-a_{331}$ do not change at room temperature or at 200°.

A slight decrease in Δa was observed in the process of heating to 300°, when the true decrease in parameter a, caused by vacancies, had practically disappeared, i. e. there occured a restoration of the parameter to an equilibrium value. Only annealing at 600° for 20 minutes caused $\Delta a=a_{420}-a_{331}$ to fall within the limits of experimental error. All the interface distances took on equilibrium values due to complete healing of all packing defects.

We note in conclusion that such high concentrations of hardened vacancies as were discovered in our investigation (from 0.29 to 0.40%) have never before been observed in works on hardening of vacancies [8]. The equilibrium concentration of vacancies at the melting point is only 0.01-0.1%. The usual methods of hardening from the solid state fix only a small portion of these vacancies -- 0.001-001% [8 -- 10].

However, these figures cannot refute the experimental data of our work. The fact is that all the experimental works cited below [7 -- 11] of the hardening of samples were performed at low rates and from temperatures below the melting point. In the case

of spark treatment of metal, point hardening occurs, consisting of exceptionally rapid cooling from the liquid state to a temperature near room temperature, which aids in the formation of vacancies, the concentration of which greatly exceeds (by several orders of magnitude) the equilibrium concentration.

BIBLIOGRAPHY

1. L. C. Palatnik, "X-ray investigations of transformations in the surface layer of metalls which have undergone the action of electrical discharges", Izvestiya A ademii Nauk SSSR [news of the USSR Academy of Sciences], physics series, v. XV, 1951, no. 1; "Transformations in the surface layer of metal under the action of an electrical discharge," same journal, No. 4.

2. V. M. Kosevich, "Manifestation of dislocation defects in antimony through the etching method," Kristallografiya [Crystallography], 1960, issue 5.

3. N. M. Gogechkori, "Experimental investigation of the channel of a spark discharge," ZhETF [Zhurnal Eksperimentalnoy i Teoreticheskoy Fiziki, Journal of Experimental and Theoretical Physics],1951, v. 21, 4.

4. L. S. Palatnik and A. A. Levchenko, "The character of electrical erosion in monocrystals," Kristallografiya, 1956, issue 5.

5. L. C. Umanskiy and assoc., Fizicheskie Osnovy Metallovedeniya [The physical Bases of Metal Science], Moscow, metallurgy publishers, 1955.

6. K. H. Benneman and L. Tewordt, "Gitterdeformationen um Zwischengitteratome, Leerstellen, Zwischengitteratom-Paare und Fenkel-Paare in Kupfer," Z. Naturforsch, 1960, Bd. 15a, N 9.

7. B. E. Warren and E. P. Wazekois, "Stacking faults in cold worked alpha-brass," Acta metallurg., 1955, v. 3, N 5.

8. "Vacancies and other point defects in metals and alloys," Tr. Konferentsii [Conference Tr.], Moscow, Metallurgy publishers, 1961.

9. B. G. Lazarev and O. N. Ovcharenko, "Energy of formation and transference of vacancies in gold and platinum," ZhETF, 1959, v. 36, 1.

10. R. O. Simmons and R. W. Balluffi, "Measurements of the high-temperature electrical resistance of aluminum: resistivity of lattice vacancies," Phys. Rev., 1960, v. 117, N 1.

11. R. O. Simmons and R. W. Balluffi, "Measurement of the equilibrium concentration of lattice vacancies in silver near the melting point," Phys. Rev., 1960, v. 119, N 2.

6508
CSO: 1879-D/PE

RESIDUAL STRESSES AND DURABILITY IN HEAT-RESISTING MATERIALS AFTER SPARK TREATMENT

[Following is a translation of an article by V. P. Aleksandrov in the Russian-language book Elektroiskrovaya obrabotka metallov (Electrospark treatment of metals), Moscow, Academy of Sciences, USSR, 1963, pages 113-118.]

As is known, the technological characteristics of the electrospark treatment of metals, including heat-resisting alloys, include the pulse characteristics (energy contained, length) and repetition frequency [1,2].

A published work [3] contains the results of experiments on the workability of heat-resisting nickle alloys by pulses with varying characteristics (energy and length). It is shown that the pulse length determines the state of the surface layer in heat-resisting alloys. If the alloys are subjected to pulses over 250 usec long with energies of 0.2-4.5j, microcracks are formed in depth from the surface along grain boundaries. Local spectral analyses also showed that the fused surface of the metal has a changed chemical composition and altered physico-chemical properties. In particular, the fused surface layer has higher microhardness. The depth of the fused layer increases with pulse length (fig 1).

However, this work did not state the causes of the defective layer formed when heat-resisting alloys are treated by long pulses. They also failed to examine the question of the effect of pulse characteristics on the durability of the alloys. This work is concerned with these questions.

As is known, the surface layer of the materials in question has a cast structure after spark treatment.

With very high cooling rates, the processes of crystallization of phase transitions and diffusion lead to the formation of non-equilibrium structures in the metals and alloys. Also, high cooling

rates, as a rule, result in the formation of great internal stresses in the metals and alloys. Considering the influence of the pulse length on the depth of the fused layer which remains after processing, we would expect a dependence of the stresses in the surface layer and the depth of their penetration on the length of the electrical pulses. Investigation has shown that such a dependence does indeed exist.

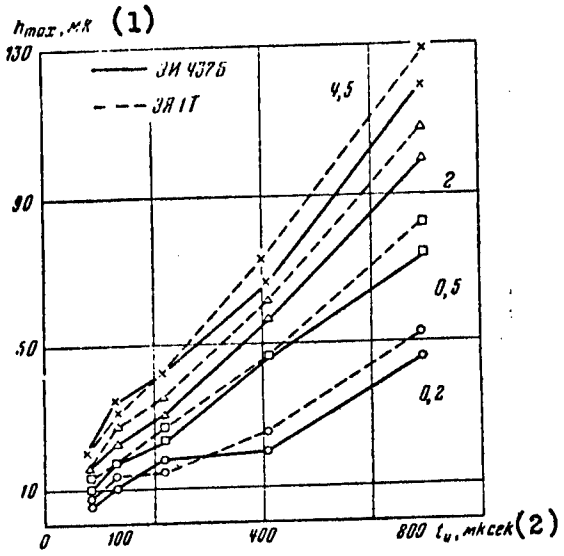

Figure 1
Maximum depth of fused layer plotted against pulse length.
Key: 1, depth, microns; 2, pulse length, μsec.

In previous works, the residual stresses have been determined by the method of academician N. N. Davidenkov [4,5,6].

In figure 2 are shown the relations of stresses in the surface layer of alloy EI437B in the depth of the layer in samples treated by pulses with energies ω_p=0.1 and 0.2 j and pulse lengths t_p=130, 480 and 1050 μsec.

As follows from the data in figure 2, stretching stresses arise in the surface layer after electrospark treatment, changing at a certain depth (depending on the alloy) to compression stresses. The stress level depends essentially on the pulse length. For example, with an energy level in the pulse of 0.2 j and a pulse length of 1050 microseconds, the stretching stress reaches 90 kg/mm^2. The stress decreases with decreasing pulse length, and at a pulse length of 130 μsec, does not exceed 40 kg/mm^2. Analogous results were obtained in treating alloy type EI617.

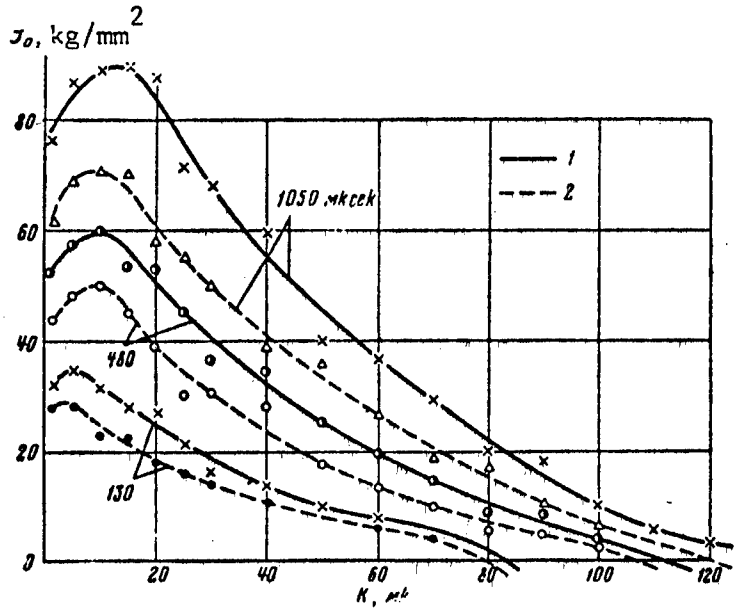

Figure 2.
Residual axial stresses in depth against pulse length. Anode -- EI4375; cathode -- Brass type LS-59. 1, W_p=0.2j; 2, W_p= 0.1j.

The formation in the layer of residual stretching stresses can be explained thus. A portion of the fused metal, remaining unseparated from the treatment zone, is reduced in volume in the transition from the liquid to the solid state. This decrease in volume is resisted by the surrounding areas of the slloy, which have lower temperature. As a result, stresses are formed in the solidifying surface layer. Thus, at great pulse lengths, stretching stresses are formed which exceed the flow limit and are near to the strength limit of alloys type EI437 and EI617.

If we consider that the surface layer has reduced ductility in comparison with the main volume, then its resistance to the action of stretching stresses is also less. This explains the appearance of microcracks in the surface layer during electrospark treatment of type EI437 alloys, as well as of type EI617, by pulses of over 250 μsec length.

Stretching stresses also arise in the surface layer during electrospark treatment of EYaIT steel. However, their level is much less than with alloys type EI437. This can be explained by the formation of the α-phase in the surface layer, which is accompanied, as is known, by an increase in volume.

With the lower residual stress level of the surface layer of type EYaIT steel, the microtrenches in the surface layer are not present, even when treatment is performed with pulses of great length and energy.

In order to clarify the influence of the above mentioned changes in the surface layer of the material under investigation on their mechanical properties, experiments on their prolonged durability were performed. The evaluation of the influence of the parameters of the pulses in the electrospark treatment on the durability of the treated materials was performed by experimental comparison of samples treated by the electrospark method and by cutting. The experiments were performed at t=700° on a type VIAM instrument. Stresses acting during the experiments were: for type EI437 alloys -- 36 kg/mm^2, for EYaIT steel -- 13 kg/mm^2. The results of the experiments are shown in table 1.

Table 1

Time to Breakdown in Hours

Material	Mechanical treatment	Electrospark Treatment					
		t_p=130 usec		t_p=480 usec		t_p= 1050 usec	
		w_p=0.2j	w_p=0.5j	w_p=0.2j	w_p=0.5j	w_p=0.2j	w_p=0.5j
EI437B	180	180	178	162	150	142	130
EYaIT	100	102	100	98	97	98	97

The experimental results showed that the pulse length essentially influences the durability of alloy EI437B.

Electrospark treatment with pulse lengths less that 250 μsec did not cause a change in the durability of EI437B alloy in comparison with the initial samples as treated by cutting. Samples treated with discharges of 480 μsec pulse length showed a reduction in durability on the order of 10-15%, whereas samples treated with 1050 μsec pulses showed durability reductions of 20-30%. Similar results were obtained for EI617 alloy. In treatment of EYaIT steel, the pulse length was found to have practically no effect on the durability. The great reduction in durability of EI437B alloy after treatment with pulses over 250 μsec is explained by the formation of microcracks in the surface layer.

In order to more fully clarify the influence of impulse characteristics on the durability properties of the metals investigated, fatigue resistance tests were performed according to state standard (GOST)2860-45. The influence of the impulse characteristics on fatigue resistance was evaluated by a comparison of the spark treated samples with

samples treated by grinding and subsequent vibration polishing. The results of experiments on EI437B alloy are shown in figures 3 and 4.

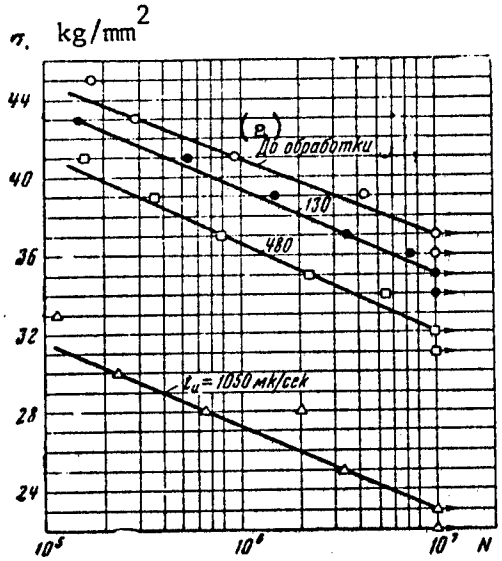

Figure 3
Strength curves of EI437B material after treatment with pulses of various lengths. a) untreated.

From the data of figure 3 it follows that the strength limit of samples which have undergone elextrospark treatment is essentially dependent on the pulse length. Whereas the strength limit of EI437B before treatment was 37 kg/mm^2, on the basis of a 10^7 cycle experiment, after treatment with impulses of 1050 μsec length it was lowered to 23 kg/mm^2, i. e. a reduction of around 30%. A reduction in pulse length resulted in an increase in the strength limit. Thus, on the same basis, the strength limit for EI437B alloy treated with 480 μsec pulses was 32 kg/mm^2. Again on the same experimental basis, treatment with 130 μsec pulses lowered the strength limit to only 35 kg/mm^2. However, even with t_p=130 μsec, the strength limit was lower than that of the inital samples.

The significant reduction in fatigue resistance in EI437B alloy when treated with pulses of great length (over 250 microseconds) is confirmed by the conclusions of metallographic investigations [3]. It is natural that the presence of microcracks in the surface layer of material like alloy EI437B cannot fail to lead to significant reductions in strength limit.

The slightly lower strength limit of the material treated by pulses of less than 250 microsecond duration (with t_p=130 microseconds,

σ_{-1} = 35 kg/mm^2 in comparison to the initial value of σ_{-1}=37 kg/mm^2) can be explained as follows. First, after electrospark treatment, there are rather strong stretching stresses in the surface layer of the metal. Also, the fused surface layer is to a certain extent saturated with the gasses which are the products of the decomposition of the inter-electrode fluid under the influence of the pulsed electrical discharge. Experiments [7] have shown that these gasses contain unsaturated hydrocarbons up to 28%, and up to 72% hydrogen.

Many works [8,9] contain data testifying to the negative influence on fatigue resistance of hydrogenation of the surface of the metal in the process of application of various coatings.

Thus, the certain slight reduction in fatigue resistance during electrospark treatment of alloy EI437 by short pulses must be attributed to residual stresses in the surface layer and to the gas saturation of the fused surface layer, lowering the resistance to fragility of the metal.

In order to determine the minimal allowance necessary for restoration of the strength limit to its initial value, we performed another series of gatigue experiments.

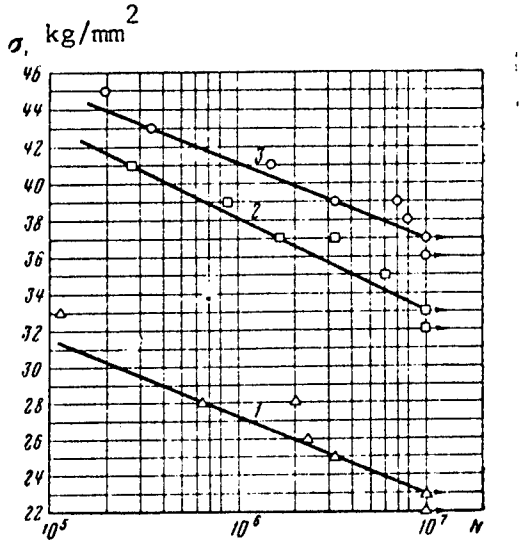

Figure 4.
Strength curves for EI437B material after treatment with 1050 usec pulses; W_p=0.2 j. Key: 1,without separation of layer; 2, with separation of layer to 0.1 mm; 3, with separation of layer to 0.2 mm.

From the results of these experiments (see figure 4) it follows that the removal of a layer of 0.1 mm by grinding with subsequent polishing after electrospark treatment with impulses of length 1050 μsec (in this case $R_z + T \approx 0.1$ mm) did not result in restoration of the strength limit to its initial value. This is explained by the deep penetration of the cracks below the fused layer. Therefore, some of them remain in the surface layer even after the removal of a 0.1 mm allowance by grinding and polishing. The strength limit is restored to its initial value only after removal of a layer of 0.2 mm.

For samples treated with 130 microsecond pulses (in this case, $R_z + T \approx 0.035$ mm), removal of a layer 0.04 mm thick was seen to be sufficient to restore the strength limit to its initial value. The minimal necessary allowance for final processing is determined by the following formula:

$$z_{min} = R_z + kT,$$

where R_z is the average microcrack depth; T is the depth of the fused layer; k is a coefficient taking the state of the surface layer into consideration.

When treating with impulses of less than 250 μsec length, k=1. When treating with impulses over 250 microseconds in length, k equals approximately 2.5.

The above indicates that the pulse characteristics, especially the pulse length, have essential influence on the fatigue resistance of type EI437 heat-resisting alloys.

Analogous qualitative results were obtained for alloy EI617.

Using long pulses (over 250 μsec) for treating these alloys makes necessary a significant increase in the allowance for final processing.

BIBLIOGRAPHY

1. B. P. Lazarenko and N. I. Lazarenko, Elektroiskrovaya obrabotka metallov [Electrospark treatment of metals], Moscow, state power publishing house, 1950.

2. B. N. Zolotykh, Fizicheskie osnovy elektroiskrovoy obrabotki metallov [Physical bases of the electrospark treatment of metals], Moscow, state technical-theoretical publishing house, 1953.

3. V. P. Aleksandrov and B. N. Zolotykh, "The selection of optimal conditions in the treatment of heat-resisting alloys based on Nickle by the electrospark method," Izvestiya Akademii Nauk SSSR [Herald of the Academy of Sciences, USSR], department of technical sciences, (Trudy Kuybyshev aviats. in-ta [Tr. of Kuybyshev aviation institute]).

4. N. N. Davidenkov and E. M. Shevandin, "Investigation of the residual stresses caused by bending," ZhTF [Zhurnal Tekhnicheskoy Fiziki, Journal of Technical Physics],v. 9, 12, 1937.

5. N. N. Davidenko, "The design of curved beams," Prikhladnaya matematika i mekhanika, [applied mathematics and mechanics], v. 1, 3, 1933.

6. V. P. Aleksandrov, V. E. Loginov and A. N. Nikitin, "A study of residual stresses in the surface layer during processing of heat-resisting and titanium alloys," Izvestiya Vyshykh Uchebnykh Zavedeniy aviats. tekhnika [Aviation Technology Institute of Higher Education News], No. 2, 1961.

7. N. S. Pechuro, A. N. Merkurev, E. Ya Grodzinskiy and N. I. Sokolova, "An investigation of the physico-chemical changes which take place in organic media under the influence of electrical discharges," in the book Problemy electricheskoy obrabotki materialov [Problems in the electrical processing of materials], Moscow, 1960. (trudy TsNII-ELEKTRON [Central science-research laboratory for Electro-mechanics]).

8. S. I. Ratner, Razrushenie pri povtornikh nagruzkakh [Breakdown under repeated loads], Moscow, oborongiz [state defense publishing house], 1959.

9. Ya. M. Potak, Khupkie razrusheniya stali i stalnykh detaley [brittle breackdown of steel and steel parts], Moscow, Oborongiz, 1955.

6508
CSO: 1879-D/PE

MACROSCOPIC STUDY OF CHANGES IN THE STRUCTURE OF THE SURFACE LAYER OF STEELS AND ALLOYS AFTER ELECTRICAL DISCHARGE CUTTING

[Following is a translation of an article by I. Z. Mogilevskiy, Ya. L. Linetskiy and S. A. Chepovaya in the Russian-language book Elektroiskrovaya Obrabotka Metallov (Electrical Discharge Treatment of Metals), Academy of Sciences Publishing House, Moscow, 1963, pages 119-125.]

It has been noted more than once that during electrospark treatment of metals and alloys, stong changes in the surface layers take place [1-3]. In this article, we will analyse the results of macroscopic investigation of the structure of the surface layers of samples of steels and several nickle-based alloys after cutting on an electrospark cutting tool with a rotating electrode disc of soft steel [4].

The cutting disc had a diameter of 500 mm and a thickness of 1.5-2 mm. The movement of the disc was automatically regulated. The power supply for the tool was, in almost all experiments, a reduction transformer, connected to a full-wave selenium rectifier. For comparison, in some of the experiments the tool was supplied by a model GS-500 DC welding generator with independent excitation and a separate degaussing coil.

During operation, the average voltage at the gap and the average working current were measured (see tables 1-3). The working current varied from ±30 to ±40 a, and the voltage from ±2 -- 3 v, while working in the coarsest conditions. Sometimes, due to a particle of the material falling into the cutting zone, or as a result of a short circuit between the disc and the work, the current reached ±50--70 a and the voltage, up to ±3--5 v.

The working fluid used was suspended kaolin, consisting of an aqueous solution of 50 g/l boric acid, 40 g/l borax and 450 g/l crushed

kaolin. The working fluid was cooled, and its temperature during the experiments was maintained within limits of 20--25°.

Shims were cut from the rods investigated (see fig 1,a) with a thickness of 10--15 mm. Each shim was cut through the horizontal diameter of the circle; a microsection was prepared in the plane of the cut (fig 1,b). A number of the shims were cut along vertical chord and diameter for investigation of the structure in the direction of lowering of the disc (fig 1,c). Also, broken sections of the shims were investigated.

The macrostructure of the surface of the shims was revealed by etching. This macrostructure had three zones: the central zone, and two outer zones which were of another color. The outer zones were zones of thermal influence.

Investigation of the macrosections after cutting of rods of 35KhGSA steel showed that under the same conditions, the length of the outer zones was almost identical in thick and thin shims, but the thickness of the outer zones was somewhat greater in shims of greater thickness; this difference was not found with shims of over 10 mm thickness.

The following steels were investigated:
perlitic class -- steels 45, 35KhGSA, U9, U10, KhG, 9KhS, KhVG;
martensite class -- hypoeutectoid 18KhNVA and ledeburite Kh12F, R18, R9;
austenitic -- G13, 1Kh18N9T;
and chrome-nick alloys Kh20N80 (EI435), EI617.

To show the macrostructure of carbon and alloyed steels, we used etching with the following solutions: 2.5 g $FeCl_3$ + 12.5 ml HCl + 25 ml ethyl alcohol 3% HNO_3; 5% HNO_3; the macrostructure of alloy EI617 was clarified by electrolitic etching in a 0.1% solution of hyposulfite with the following conditions: I=0.15 a/cm^2, E=35 v, t= 15 sec; steel type 1Kh18N9T and alloy Kh20N80 were etched with an agent of two parts by volume HNO_3 and 3 parts by volume HCl plus $CuCl_2$ to saturation.

The results of cutting samples of 35KhGSA steel and hardened steel U9 are shown in tables 1--3.

The experiments showed that the quality of the surface of the cut decreases with an increase in the voltage -- roughness and traces of fusion appear. During macroscopic investigation of the surface section in any direction (across the diameter of a separated shim or along any chord) there appears a thin shiny layer of uneven thickness. This layer is present under all cutting conditions: the thickness of the layer is 0.05--0.15 mm; local areas are encountered as thick as 0.3 mm; in some places, especially near the output of the disc, this uneven layer is not observed.

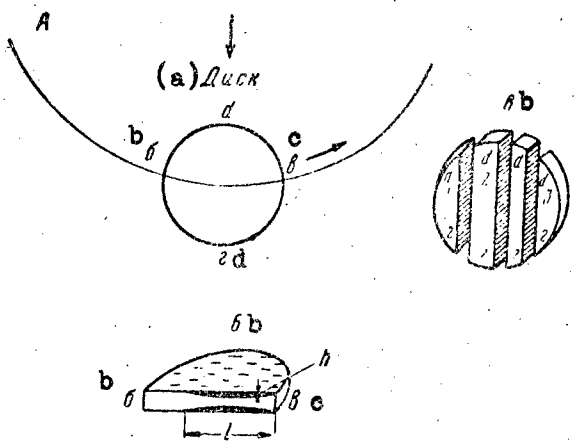

Figure 1.
Plan for cutting and preparation of samples. a) disc

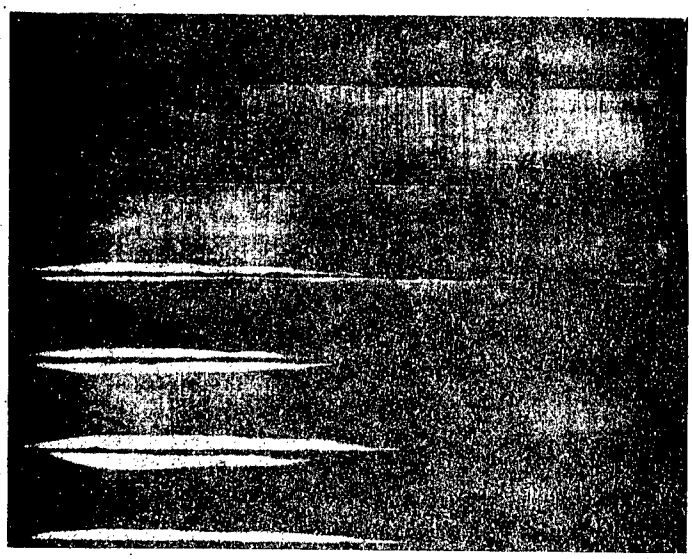

Figure 2.
Macrostructure of samples of steel 35KhGSA, cut from a rod of ∅ 95 mm (see table 1,2,3--400a; 4,5--500 a; 6,7--600a; 8,9--700a;10,11,12--800a).

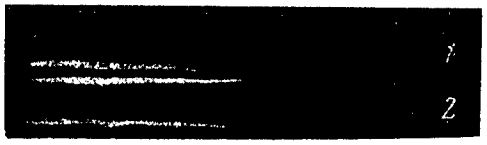

Figure 3.
Influence of peripheral velocity of rotation of disc on the dimensions of the thermal influence zones: sample 1, peripheral velocity of disc 9 m/sec; sample 2, 30 m/sec.

Figure 4
Macrostructure of samples of steel U9, 1--200 a, 23 v; 2--300 a, 22-23v; 3--400 a, 23-24v; 4--500 a, 22-23 v; 5--600a, 23-24 v.

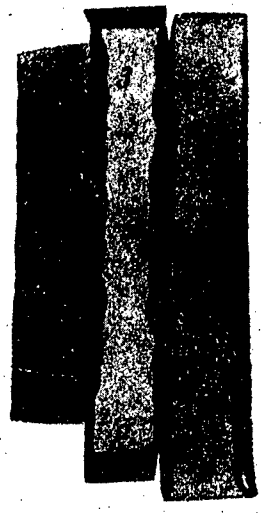

Figure 5
Macrostructure of vertical section of shim of steel KhG. I=[illegible]00a,E=22 v; marking of points on samples matches figure 1,c.

Changes in the macrostructure after cutting at currents of 100, 200, 300 a were limited to the appearance of the indicated thin surface layer.

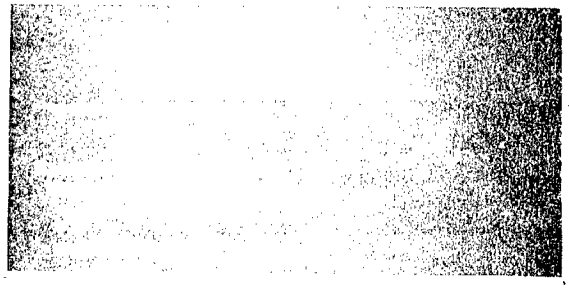

Macrostructure of [illegible] steel. 1, 400 a, 21 v;
2, [illegible] a, 22 v.

A crack in a [illegible] rod of 45 steel.

Macrostructure of a [illegible] of U10 steel, cut from a rod ϕ 70 mm, [illegible].

When coarser conditions are used (400--1,000 a), significantly deeper strips of tapered form appear near the cut surface, their color depending on the etching agent used. Each outer zone in this case consists of two bands: a very thin light band, running almost along the entire section, and a much deeper band of tapered form.

Table 1. Dimensions of thermal influence zones in rods of 35 KhGSA steel
Power supply: reducing transformer with selenium rectifier. Average working voltage 21--23 v; peripheral rotating velocity of disc, 20 m/sec.

(c) $I_{ср}$, а	Ø 30 мм		Ø 60 мм		Ø 69 мм	
	(a) толщина слоя, мм	(b) длина слоя, мм	(a) толщина слоя, мм	(b) длина слоя, мм	(a) толщина слоя, мм	(b) длина слоя, мм
100	0,1	30	0,1	60	0,1	95
200	0,1	30	0,1	60	0,1	95
300	0,5 *	14	0,1	60	0,1	95
400	0,65 *	18	0,8 *	23	0,1	95
500	1,3 *	20	1,4 *	46	0,1	95
600	1,5 *	20	1,7 *	48	1,4 *	52
700	—	—	1,8 *	48	1,7 *	50
800	—	—	2,2 *	50	2,5 *	57

Key: a) layer thickness, mm; b) layer length, mm; c) I_{av}, a;
*zone of fusion and thermal effect.

At the point of initial disc entry in the rod, the second band is absent; it appears approximately at the middle of the cross section of the rod (fig. 2) and continues, constantly broadening, to the final contact point. At the final contact point, the thickness of the band reaches a maximum, after which it decreases. With the form of the bands as shown in the macrosections, we will characterize their maximum thickness as h and length as l.

Experiment showed that increases in current and voltage causes increases both in h and in l for all the structure-changing zones. The thickness and length of the zones with the came operating conditions vary within limits of ±15%.

The data shown in tables 1--3 show that when the welding generator is used as a power supply, deeper tapered bands result. However, it must be kept in mind that in all the printed tables, the average current values are shown. It is known that with the same disc feed

rates and productivity, but with power supplied by different sources, the average current values will be different, although the actual values will be the same.

Table 2. Dimensions of thermal influence zones in rods of 35KhGSA steel of 60 mm diameter

Power supply: DC generator type GS-500 with independent excitation and separate series demagnitizing coil. Average working voltage 21--23v, peripheral rotating velocity of disc, 20 m/sec.

$I_{ср.}$ (c)	(a) Толщина слоя, мм	(b) Длина слоя, мм	$I_{ср.}$ (c)	(a) Толщина слоя, мм	(b) Длина слоя, мм
100	0,1	60	500	1,7 *	35
200	0,1	60	600	1,9 *	47
300	0,7 *	25	700	2,1 *	50
400	1,4 *	27			

Key: a) layer thickness, mm; b) layer length, mm; c) I_{av}, a; *zone of fusion and thermal effect

Table 3. Dimensions of thermal influence zone in rods of U9 steel

Average working voltage 22--24 v; peripheral rotating velocity of disc, 20 m/sec.

(e) $I_{ср.}$ a	(a) Понижающий трансформатор и выпрямитель		(b) Сварочный генератор постоянного тока	
	(c) Толщина слоя, мм	(d) Длина слоя, мм	(c) Толщина слоя, мм	(d) Длина слоя, мм
100	0,1	30	0,1	30
200	0,1	30	0,1	30
300	0,1	30	0,5 *	15
400	0,8 *	18	1,6 *	19
500	1,9 *	17	1,7 *	24
600	2,1 *	25	—	—

Key: a) reduction transformer and rectifier; b) DC welding generator; c) layer thickness, mm; d) layer length, mm; e) I_{av}, a; * zone of fusion and thermal effect.

The diameter of the rod being cut also influences the form of the structurally-changed zones: h decreases with increasing diameter. Thus, in macrosections of a rod with ϕ 95 mm of 35KhGSA steel, these zones appear only after cutting with a current of 600 a; even then, these zones have lesser depth than with rods of the same steel but of smaller diameter. The zone length depends on the rotating speed of the disc.

On figure 3 are shown macrophotographs of shims of 45 steel, ϕ 60 mm after cutting, (500 a, 22 v) with a peripheral rotation velocity of the disc of 9 and 30 m/sec. In the first case, the ratio of the length of the band to the diameter of the rod is 0.8, in the second, to 0.6; the length of the structure-change zones decreases with increase in the rotation speed of the disc. The dependence of the thickness of these zones on the velocity of the disc is less strongly expressed; apparently it decreases somewhat with increasing rotation velocity.

Let us analyse in greater detail the macrostructure of the samples cut from rods with ϕ 30 mm of hardened steel U9 (see table 3).

At the edges of these samples (fig 4) can be seen white bands, in the shape of a section of a cylinder, embracing the entire rod. Their thickness is on the order of 5--6 mm. These bands have no relation to the cutting process; they are formed as a result of the preliminary hardening of the rods are zones of complete hardening of the U9 steel.

During cutting, the structure of these bands was changed in the following manner. In the sample, cut at 200 a, 23 v, the ring zone of complete hardening remains white after etching. Under coarser cutting conditions (300 a, 23 v), at the exit point of the disc (point c, fig 1) this ring zone is bordered by dark strips from both sides from the surface of the cut to a depth of 2--3 mm, with the thickness of the darkened zone decreasing toward the edge. A similar, but very weak, darkening of the entrance side of the cut (point b, fig 1) was observed only with samples cut at the very coarsest regimes.

Also, after cutting at 400--600 amps, the cutting surface of the hardened samples showed light tapered bands similar to the bands observed in cut samples of non-hardened steels.

In order to establish the configuration of the zones of thermal influence, we studied the macrostructure in vertical sections of the shims, that is in the direction of feed of the disc. On fig 5 are shown the structure of three macrosections of samples of KhG steel. It can be seen that the zone of thermal influence has maximum thickness at the region of the horizontal diameter of the rod, not far from the point of the exit of the disc (see fig 5, macrosection 3).

At the upper and lower points of the cut rod, i. e. at the beginning and end of the cut, the thermal influence zone is, as a rule, thinner than in the middle portion of the section. True, in some sections, at the end of the cur, in the region of the vertical diameter, a thickening of the zone is observed (see fig 5, macrosection 2).

Data on the dimenstions of the structure-change zones in cut samples of other types of steel and chrome-nickel alloys are shown in table 4.

As an example, in fig 6 we see the macrostructure of samples of Kh12F steel (rods 55 X 5[illegible]), cut at currents of 400, 600 and 800 a. First of all let us note that the macrostructure of this type does not appear with all materials: on samples of steels type 1Kh18 N9T, G13, alloy EI435, the tapered bands are absent. The latter shows the thermal nature of the formation of the bands, since it indicates that they are actually zones in which certain phase or structural transformations have taken place under the influence of heat in the cutting process. Naturally, in steels and alloys which have no phase or structural transformations upon heating or cooling, these zones should not appear. From this point of view, the dependence of the depth of the structure-change zones on the cutting conditions becomes clear: the coarser the cutting conditions, the more heat is liberated with each electrical impulse and the deeper the structure-change zone in the material

The presence of a cooled fluid in the interelectrode zone has a great influence on the thickness and the length of the structure-change zone. In the case of cutting of peices in a bath, the feed of cooling fluid to the interelectrode gap is aided by the use of a rotating disc electrode. At the very beginning of the cut, the fluid easily penetrates into the interelectrode zone, but with penetration of the disc into the peice, the feed of the fluid over the entire length of the cut becomes ever more difficult. At the entrance region of the disc into the cavity of the cut (point b, fig 1), there is a quantity of fluid present which is sufficient for intense cooling of the surface layers of the metal; with further movement of the disc from point b to point c, the penetration of the fluid in the gap is hindered by the liberated gasses; also, the stream of the fluid can be separated from the surface of the disc. As a result, an insufficient quantity of fluid is supplied to the exit region of the disc; the discharges are formed partially in a gas-droplet medium; the surface of the metal gives off greater quantities of heat, and its cooling is hindered. At the exit point of the disc (point c), the feeding of the fluid to the cutting zone is once more easier, the cooling of the metal is made much easier. In the same way, the thickness of the thermal effect zones changes: at the region of the entrance of the disc, these zones are absent; they appear near the vertical diameter of the cut rod, widen toward the exit of the disc from the rod, and near the output point, become once more thin and decrease to nought.

An increase in the rotating speed of the disc, within limits depending on the viscosity of the fluid, facilitates the supply of the liquid by the disc to the interelectrode gap, resulting in the shortening and narrowing of the structure-change zones.

When cutting thin rods (Ø 30 mm), when the supply of the fluid to the center of the cavity of the cut and the exit region of the disc is easier, the structure-change zones are found to be still rather deep and long. This is apparently explained by the fact that the discharges occur closer together, due to the comparitively small dimensions of the cavity; they occur much more often than in the case of a long cavity in a larger diameter rod. The metal cannot cool in the short interval between impulses, resulting in an increase in the depth of the heated zone in the metal.

A comparison of the thickness of tapered bands for investigated samples of construction and tool steels did not allow the selection of a group of steels for which this band is least thick. It can only be supposed that the deepest zones with changed structure (in contrast to the structure of steels of the perlitic and carbide classes) should be found in martensite steels (18KhNVA). Probably, the true depth of the structure-change zone for a number of samples (for example 18KhNVA steel) is somewhat greater than that shown in the macrosection. The trouble is that the corrosibility of some structures in the zones of thermal influence, which arise as a result of cutting, can differ only slightly from the corrosibility of the portions of the metal with the initial structure; than macroscopic investigation will not determine the exact dimensions of these structurally changed zones.

The depthsof the structurally-changed zones on samples of alloy EI617 were almost twice as small as those for samples of 18KhNVA steel from rods of the same diameter. This can be explained by the essential difference in the phase transformations which take place upon heating in these materials and the great difference in their heat conductivity and heat capacity.

The presence of zones with changed structure in samples of steel after electrospark treatment is seen also in breaks. On fig 7 are shown breaks of a sample of 45 steel, after electrospark treatment. From the photographs it can be seen that the breaks have different form in the surface layers and the central portions. The break at the surface is fine-crystalline, similar to the break in hardened carbon steel, whereas the break in the central portion is macrocrystalline.

Table 4. Dependence of thermal influence zone dimensions on average current in cutting various steels and alloys

Power supply: reducing transformer with selenium rectifier; average working voltage 21--23 v; peripheral rotating velocity of disc 20 m/sec (Ø, l and h in mm)

I_{cp}, a	9XC Ø 90		XГ Ø 70		XBГ Ø 60		P9 Ø 60		P18 Ø 60	
	h	l	h	l	h	l	h	l	h	l
400	0,8	32	0,5	35	—	—	1	35	1	30
600	1,5	46	0,8	40	1,2	34	1,8	47	2	52
800	2,8	55	2	45	2	40	2,8	52	2,5	53
1000	—	—	—	—	—	—	—	—	—	—

The zones with the fine-crystalline breaking have tapered form, the depth and length depending on the conditions of the treatment. Thus, the influence of electrospark cutting on the structure of the surface layers can be studied both in the macrosections and in the form of breaks.

The process of erosion of the metal in electrospark cutting is a periodic one. At the appearance of each separate impulse, a hole is formed, under which there is a zone of structural change in the material.

Figure 8 shows the macrostructure of a portion of a sample of U10 steel at slight magnification. It can be sharply seen that the structure-change zones in this sample consist of dark (inner) bands and lighter (outer) bands. At the edge of the lighter band can be seen small, also two-part, segment zones in a row, but sometimes overlapping. These small zones are structurally changed zones which are formed as a result of the action of individual impulses. Above these small zones, the areas of structural change from individual impulses averlap, resulting in the common zone which is observed as a tapered zone in macrosections cut under coarse conditions.

Table 4 (Continued)

Х12Ф 55×58		18ХНВА ∅ 36		1Х18Н9Т ∅ 60		Г13 ∅ 52		ЭИ435 ∅ 60		ЭИ617 ∅ 32	
h	*l*	*h*	*l*	*h*	*l*	*h*	*l*	*h*	*l*	*h*	*l*
Слой оплавлен (a)		—	—	Слой оплавлен (a)		Слой оплавлен (a)		Слой оплавлен (a)		—	—
1,5	42	1,8	31	До 0,3	60	До 0,3	52	До 0,3	60	0,75	20
2	44	2,0	32	До 0,3	60	До 0,3	52	До 0,3	60	0,8	20
—	—	2,4	32	До 0,45	60	До 0,4	52	До 0,45	60	0,9	22

Key: a) layer fused.

BIBLIOGRAPHY

1. L. S. Palatnik, "Physico-chemical transformations in metals under the action of electrical discharges," Trudy fizicheskogo otdela fiz-mat fakulteta KhGU /Tr. of physics department of phys-math faculty, KhGU (Kharkovskiy Gosudarstvennyy Universitet, Kharkov state University/, 1950, v. 2, Uch. Zap., v. XXXV.

2. I. Z. Mogilevskiy, S. A. Chapovaya, "Metallographic investigation of the surface layer in steel after electrospark treatment," Electroiskrovaya obrabotka metallov /Electrical discharge treatment of metals/, first ed., Moscow, 1957 (Trudy TsNIL-ELEKTROM /trans. of central science-research laboratory of electromechanics/).

3. I. Z. Mogilevskiy and Ya. D. Linetskiy, "Investigation of the physico-chemical changes in the surface layers of steels and alloys after electrical discharge treatment in kerosine," Problemy elektricheskoy obrabotki materialov /Problems in the electrical treatment of materials/, Moscow, 1960 (Trans. of TsNIL-ELEKTROM).

4. V. N. Kondratenko, T. I. Makeeva and S. M. Moreyskiy. Povyshenie proizvoditelnosti protsessa elektroerozionnogo razrezaniya metallov /Increasing the productivity of the process of electro-erosive cutting of metals/, Leningrad, 1958 (L. D. T. technical information bulletin No. 42, Elektricheskie metody obrabotki materialov /Electrical methods of material processing/).

6508
CSO: 1879-D/PE

INVESTIGATION OF POWDERS--PRODUCTS OF SPARK EROSION MACHINING*

[Following is a translation of an article by B. A. Krasyuk in the Russian-language book Elektroiskrovaya obrabotka metallov (Electrical discharge treatment of metals), Academy of Sciences publishing house, Moscow, 1963, pages 126-133.]

Statement of Problem and Methods of Investigation

In the analysis of phenomena occuring during the electrical discharge treatment of metals, great attention is turned to the aggregate state in which the products of erosion of the product and the electrode-instrument arrive in the interelectrode gap.

This question can be investigated by the method of metallography of the metallic powder products of erosion of the electrodes made of various alloys. Experiments, as described in essence below, were performed.

Two component alloy electrodes were made, and sparks were discharged between them with characteristics normal for the electrospark treatment of metals, supplied by RC generators in two operating conditions -- light (C=10 microfarads, V_o=120 v and I_k=4 a) and coarse (C=200 microfarads, V_o=120 v and I_k=6 a). In the liquid state, these components should be completely dissolved in each other, and in the solid state they should form in the alloy a mechanical mixture, consisting of a eutectic and excess (if the composition of the alloy is not exactly eutectic) of solid solution in relation to the eutectic. Kerosine was used as a working fluid.

* This article is written according to material contained in section 2 of a dissertation which he presented in March, 1951 at the sesion of the academic council of the metallurgy institute imeni A. A. Baykov, Academy of Sciences, USSR.

The products of the electrical erosion of these alloys can contain both components of the alloy in each particle; but they can also consist of particles of two types: a) the component present in excess in comparison to the eutectic (with a small quantity of the second component in solution) and b) particles with eutectic structure.

With a great difference in the melting points of the eutectic and the excess component, when particles of the first composition variant were found, it was assumed that the products at the moment of separation from the electrode were either in the form of a mixture of the component pairs, or a homogeneous liquid solution.

The second particle composition variant would be possible in the case when the electrical erosion took place with the separation of individual portions of the material of the electrode in the interelectrode gap in the melted state as each of the structural components was heated to the liquid state.

In our experiments, we performed electrical erosion destruction of electrodes prepared from alloys of lead and antimony, containing respectively 89; 50. 65; 12.9; 9.1 and 2.67% antimony.

The erosion products were separated by settling and washing from the kerosine and soot, after which the microstructure of these particles was studied.

Another group of similar experiments was performed with electrodes formed of an alloy of copper with lead and tin--tin-lead bronze type BrOS-10-10. This alloy did not contain the antimony, which is inclined to sublimation; in its structure were contained, in the initial state, grains of a solid solution of tin in copper and almost pure lead (materials with sharply different melting points and to a sufficient degree stable against the action of the gasses liberated during the spark discharge--products of the pyrolysis of the kerosine). Also, the microstructure of particles of the powder products of the erosion of copper and iron was investigated.

Experimental Results

The chemical compositionsof the powder products of erosion of alloys of lead with antimony are shown in table 1.

The data in table 1 show that the process of electrospark treatment of lead-antimony alloys results in the formation of powders which to a great extent are different in composition from the initial material of the electrodes.

The composition changed in the direction of reduced antimony content, with the exception of the processing of the first of the above mentioned hypoeutectic alloys, whose initial composition contained 2.67% antimony.

Table 1

Initial Antimony Content, %	Processing Conditions	Content of Antimony in Powder, %
2.67	coarse	3.12
	light	3.59
9.10	light	9.10
	coarse	5.11
12.90	light	12.80
	coarse	12.00
50.65	light	46.45
	coarse	36.00
89.00	light	85.10
	coarse	21.20

The microinvestigation of the powder particles showed the following.

Among the powder particles produced in the electrospark treatment of the lead-antimony alloy (fig 1), there is a very small quantity of particles of solid solution based on lead. The main mass of the products of erosion is made up of grains whose structure is similar to the eutectic. The same sort of picture was revealed in microinvestigations of particles of the powder obtained in the electrospark destruction of electrodes containing in the initial state 9.1% antimony (fig 2).

As chemical analysis showed, these particles could not consist of the eutectic, but rather could only be richer in lead than the normal eutectic, a mechanical mixture--a quasieutectic, produced during very fast cooling of individual microdrops of the melt, in the form of a homogeneous liquid solution.

The small quantity of particles representing the lead-rich phase (almost pure lead) in comparison with the quantity of quasieutectic particles obtained during electrospark treatment of the hypoeutectic alloys could be explained by the fact that the probability of separation of the alloy during electrical discharge destruction into particles consisting of the individual structural components with different melting points depends on the degree of difference of these points.

Since the melting points of lead and the eutectic of lead with antimony are relatively close (347 and 246°), during the action of the impulse discharge on the electrode, consisting of the hypoeutectic

alloy, the eutectic and the grains of the lead-rich excess phase contained in the initial material are fused almost simultaneously.

From the erosion-destroyed surface of the electrode, microdrops of a liquid solution with hypoeutectic composition were thrown off into the interelectrode gap. The process of difusion in this case managed to sufficiently equalize the composition of the microdrops across their section that each drop became a droplet of a homogeneous liquid solution.

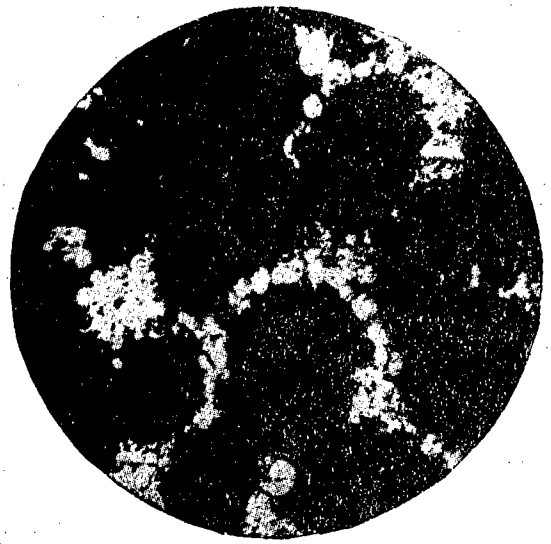

Figure 1.
Microstructure of particles of the powder obtained in the electroerosion destruction of lead-antimony alloy (antimony, 3.12%) (X 100).

Thanks to the rapid cooling of the microdrops by the kerosine, the eutectic formations in each drop of the solution was not isolated, and the quasieutectic structure resulted.

In the hypereutectic alloy of lead and antimony, on the other hand, microinvestigation revealed a significant number of particles of a powder consisting of the antimony-rich hypereutectic phase-- the solid solution. The reason for this phenomenon was the great difference in the melting point of the eutectic (246°) and the hypereutectic structural component rich in antimony, whose melting point is 631° C.

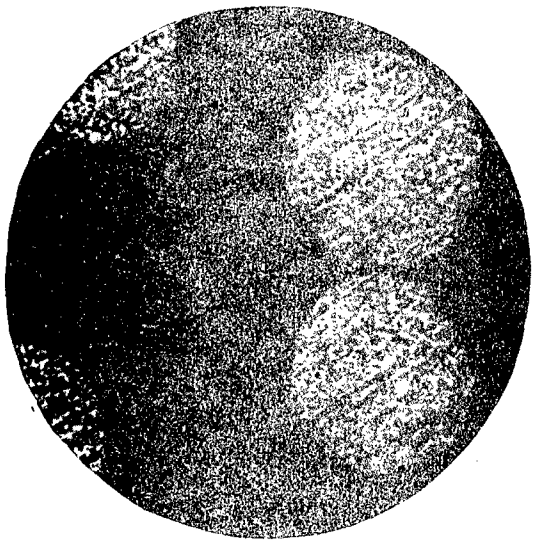

Figure 2.
Particles of powder from an alloy containing 9.1% antimony
(remainder lead; X 80)

Figure 3
Particles of antimony condensate (X 15,000)

Let us further analyse the question of the disappearance of one of the components of a heterogeneous alloy, when the chemical composition of the powder obtained by electrospark treatment is different from the composition of the crushed alloy.

A good example of this disappearance is the case of the crushing of the alloy of lead with antimony, containing in the initial state 9% antimony, in which coarse electrospark treatment yields a powder with an antimony content of only 21.2%.

It was natural to assume in the given case that a portion of the antimony disappeared due to being transformed to the vapor state; not being condensed in the form of more or less large particles, the antimony formed very small particles which formed a sort of suspension in the working fluid.

Spectral analysis of the filtered working fluid showed the presence of a significant quantity of antimony.

Electron microscope investigation of samples showed that the kerosine contained particles of antimony with rectangular crystalline form in the form of a suspension (fig 3).

As was stated, the investigation of erosion products was performed with electrodes of tin-lead bronze BrOS 10-10 containing on the average 10% tin and 10% leadas well as with electrodes of the lead-antimony alloys.

In the alloys of copper with lead, first a tiny quantity of lead can be dissolved in the solid state at room temperature. In the melts there is not full mutual solubility, and stratification of the liquid alloys is observed in them through a wide range of concentrations.

During hardening of alloys of copper with lead, containing less than 92.5% lead, at 954° crystals of almost pure copper are formed.

In alloys of copper with lead, a monotectic reaction takes place at 954°, resulting in the crystallization of the main mass of the copper; the concentration of the lead in the liquid phase increases to 92.5%.

With further cooling of the alloy, a certain quantity of copper will be additionally separated from the lead-rich remaining liquid solution, and from the crystals of the solid solution of lead in copper a certain quantity of melted crystals of the high-lead component will be separated. The alloy is fully hardened only as 326°, when the separation of almost all the copper from the melt is completed.

An alloy of the lead bronze type, cooled to room temperature, has a two-phase structure, one of the components being copper-rich

solid solution crystals, the other almost pure lead.

When lead bronze is heated, its melting begins with the transformation of the nearly pure lead inclusions to the liquid state.

The presence in the alloy of a certain quantity of tin, for example 9-10% tin as in tin-lead-bronze type BrOS 10-10 in addition to the lead and copper, does not essentially change the character of the processes described above. In BrOS 10-10 bronze, the high-copper phase in the solid and liquid state contains the third component, tin, in solution; the temperature of its transformation from the solid to the liquid state, and back, are somewhat altered in comparison with the temperatures of the liquidus and solidus curves for the analogous binary copper-lead alloy.

In analysis of the powder particles of the erosion product of tin-lead bronze it was seen that its chemical composition is close to that of the initial electrode material. Almost the entire mass of the erosion products sould be separated from the working fluid (kerosine) by settling and filtering. This allowed the supposition that the quantity of the products of erosion of the material of the electrodes depends in electrospark treatment on the tendency to sublimation of the components of the alloy from which the electrodes are made.

In separating the products of erosion of tin-lead bronze, the naked eye can distinguish separate shiny scales. In places, these scales were seen among other, smaller powder particles -- products of erosion. Microinvestigation showed that these scales were particles of the crystals of the high-copper phase which had not been fused. The scales were shiny, since on their surface clearly appeared breaks along the planes of cleavage of the crystalls.

The mechanism of formation of the scales can be represented thus.

Under the action of the discharges on the electrode made of tin-lead bronze, local heating caused first of all the fusion of the inclusions of the easily melted component of the alloy in the heated zone -- the lead-rich phase. Further, the grains of the copper rich phase in the heated zone were melted, first of all near the locations of the inclusions of the high-lead phase.

The sudden thermal expansion of the heated particles of the hard-to-melt phase in combination with the forces acting on the eroding electrode, in the area near the "spot" of the discharge, created in some parts of the material of the electrode stresses sufficient for mechanical breakoff of particles of the solid phase from the crystals of the solid solution, rich in copper. These particles fell into the working fluid without having been heated to a temperature sufficient for melting.

Microinvestigation of powder particles -- products of the electrical erosion of comparitively infusible metals (copper, bronze, iron, nickel, etc.) has shown that a certain quantity of these particles are hollow. Together with the whole particles in the products of electrical erosion of the above-mentioned metalls and alloys, parts of individual hollow particles are found. The general character of the structure of the hollow powder particles can be seen on microphotographs (figs 4, 5, 6).

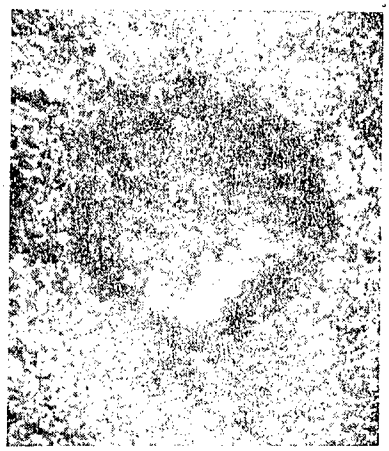

Figure 4.
Section of a hollow inside a particle of Bronze
(X 00)

Figure 5.
Section of a particle of copper powder
(X 500)

The relative quantity of hollow particles in powders in many cases can be rather great; in copper powder produced by electrical discharge, for example, it can be 10 to 30% of the overall quantity of particles in a powder sample.

The presence of hollow particles among erosion products we explained thus. It can be assumed that a part of the gasses liberated in the interelectrode gap as a result of the action of the discharge on the working fluid under great pressure is dissolved in the microdrops of metal present in the interelectrode gap. The particles thrown from the body of the electrode are rapidly cooled and in some of them cavities of the shell type remain.

When a microdrop of metal in the interelectrode gap begins to cool, the pressure of the surrounding gasses is reduced; then the small gas bubbles in the microdrop greatly increase in volume.

However, the interaction of the gas phase and the microdrop of melt thrown off in the interelectrode gap may not be limited to solution of the gasses in the melt.

Gasses separated in liquid media during electrical discharges can, as we discovered, react with the material of the surface layers of the electrodes and with the products of electrical erosion of the metals. Especially, for example, in 1945 we established the possibility of cementing, nitrating or diffusion alloying the surface layers of the material of metal products with various elements. During such electrospark alloying of metal, the elements which were to saturate the surface layers of the materials of the products had to be present in the working fluid used as a medium for processing (see the description of author's certificate No 70270, 16 January 1946, issued to B. A. Krasyuk and B. R. Lazarenko).

As a result of the chemical interaction of particles of the erosion products of iron with the gaseous products of pyrolysis and cracking of kerosine, the iron powder produced by the electrical discharge method in kerosine or mineral oil was always found to be somewhat carburized. The carburization can be prevented by using as a working fluid a mixture of a hydrocarbon with certain other additives, if gasses are formed by the electrical discharge which have no cementing action.

Conclusions

1. During the electrical discharge treatment of metals, the erosion products are present in the discharge gap partially in the vapor state, sometimes (in small quantities) in the form of solid particles, mechanically separated from the electrodes, and mainly in the form of microdrops of fused metal.

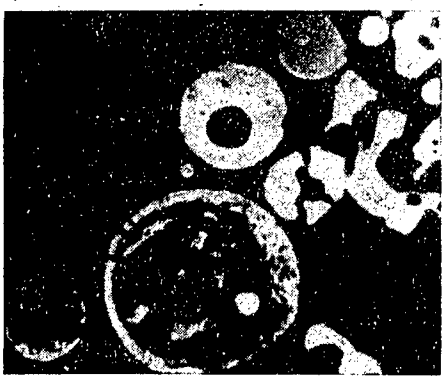

Figure 6.
Section of particles of iron powder (x 300).

2. The process of vaporization of electrodes made of metal alloys takes place selectively during electrical discharge treatment, primarily in the components of the alloy which are more inclined to sublimation. The chemical composition of the powder products of erosion as separated from the working fluid by settling and filtration are different from the initial composition of the material of the eroded electrodes: the erosion products are relatively richer in the component or components least inclined to sublimation.

3. If the individual structural components of the electrode material have similar melting points, intense diffusion will take place in the micro-drops in the time interval between local melting of the electrode and the beginning of crystallization of the micro-drops in the working fluid. In this way, the microdrops of liquid solution can become homogeneous.

4. If the melting points of the individual structural components of which the electrodes are made are sharply different, the powder erosion products will consist mainly of particles of the individual structural components of the initial materials of the electrodes.

5. During electrical discharge treatment, ejection of at least a part of the melt from the heated zone on the electrode, occurs in the presence of high-pressure gasses, which act on the melt.

For this reason, the melt can contain large quantities of dissolved gasses, and the gas bubbles which form in some micro-drops are able further, with reduction of the pressure in the interelectrode gap, to transform these cooling particles into thin-walled, hollow metal spheres.

6. The composition of the surface layers of the particles thrown off in the discharge gap can be changed due to their chemical interaction with the gas phase which fills the interedectrode gap at times. By changing the composition of the liquid medium it is possible to change the composition of the gas phase which is formed in the vicinity of the discharge channel in some desired direction. It is thus possible to influence the results of the unique gas chemical-thermal processes which are undergone by the particles of the erosion products.

6508
CSO: 1879-D/PE

ION BEAM DRILLING

[Following is a translation of an article by V. K. Popov and M. N. Kalinychev in the russian-language book Elektroiskrovaya Obrabotka Metallov (Electrical Discharge Treatment of Metals), Academy of Sciences publishing house, Moscow, 1963, pages 161-166.]

Introduction

The most widely used method of producing holes of diameter over 100 mm is the electrical discharge method [1]. Its usage for the production of holes with diameter less than 30 microns is difficult. The production of holes less than 25 microns in diameter is as yet impossible due to the low rigidity of the electrode instrument, which is in this case a thin wire. Also, electrical discharge treatment is performed in a medium of kerosine, requiring chemical cleaning of the treated parts, which leads to increases in the hole diameters.

The following technological approach is sometimes used to obtain very small hole diameters: electrical discharge treatment is used to produce a hole 50-60 microns in diameter, which is then reduced to 18-30 microns by deposition. This method can be used only for the production of individual holes in rather ductile materials.

The method of chemical etching [2] is usable only for thin foils and requires very exact preparation of the working instrument for deformation -- the diamond indentor. The minimum diameter hole which can be produced by this method is 4 microns. It is fully obvious that the usage of chemical atching for the production of holes on the order of several dozens of microns is inexpedient, due to the etching of the part itself, and in thick parts is completely impossible.

It is known that a well-focused ion stream, directed at the surface of metal can produce a depression, and if the metal is thin enough, a hole [3]. The destruction of the material (treatment) in this case is performed by ions of gas, focused and accelerated by a

strong electrical field. This principle is the basis for the hole-cutting apparatus shown in figure 1. The minimum diameter of hole which can be cut on this machine is equal to 5 microns.

Principle of Operation and Power Characteristics of the Ion Gun

At the basis of the treatment process is the phenomenon of cathode thermionic emission. In the given construction, the so called gas discharge is used [4], which exists only in a definite range of pressures and high potential difference. The principle of operation and construction of the ion gun can be seen in figure 2.

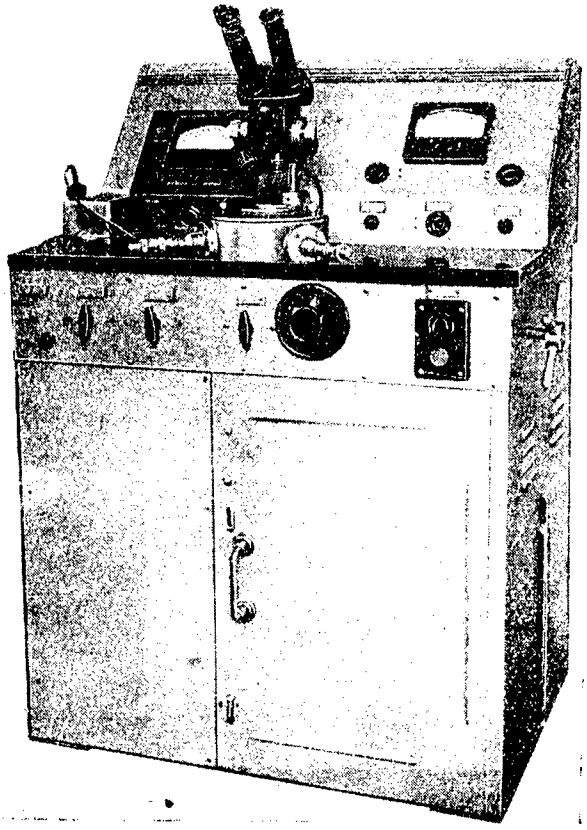

Figure 1
Apparatus for ion production of micron holes.

The ion gun is a dielectrode optical sistem, in which anode 1 has a cavity which is the ion source, and cathode 2 has a round aperture for the outflow of the ions. The part to be treated 3, which is under the cathode potential, closely adjoins the cathode surface. The dimensions of the aperture in the anode are so selected that its length is at least three times its diameter, and the ratio of the aperture diameter to the diameter of the outflow aperture is within limits of 1--3. Ionization of a molecule of gas is performed by electrons which arise as a result of cold emission from the cathode. The distance between the planes of the cathode and anode is such that at the given gas pressure it is less than the free path of the electrons. Therefore, no discharge occurs in the area between the cathode and anode. The electrons which arrive in the anode aperture ionize the gas molecules, since the length of the electron free parh is less than the path which it would have to travel to arrive at the walls of the aperture. Consequently, the anode aperture is a sort of ion source. Since the coltage between the electrodes is 0.5--15 kv and the strong electrical field penetrates deeply into the aperture, the ions are extracted from the aperture, are accelerated and, passing through the space between the electrodes, are focused in a very narrow conical beam with a focal point above the cathode. As a result of the ion bombardment on the part, a small conical hole of parallel form with a shiny inner surface is formed, the inner surface corresponding to class 9--10 cleanliness.

Since the destruction of the material is performed by gas ions, it is obviously necessary to know the electrical parameters of the ion gun and their connection with the productivity of the operation.

The magnitude of the total ion current will be determined by the state of the interelectrode gap, i. e. the gas pressure and the intensity of the ionizer. To elucidate the character of the discharge, it is necessary first of all to know the volt-ampere characteristics. In taking the characteristics, it is necessary to consider the current distribution (fig 2). The portion of the current which flows through the anode-part circuit is the working current. Only the ions which hit the part perform useful work in the puncturing of the material.

The total current will include both the working current and the portion of the current which is cut off at the cathode. The volt-ampere characteristics, shown in fig 3, were taken only in the pressure range in which hindered thermionic emission takes place. (On all graphs, the pressure in the chamber is shown in divisions of the middle scale of the VT-2 vacuumeter.) As can be seen from fig 3, at assigned constant pressure there is a direct proportional dependence between the working current and the coltage on the gun. The lower the pressure in the chamber, the more sharply the characteristics change. At a vacuum approximately equal to 0.5 mm Hg (7 and 9 divisions on the vacuumeter),

the voltage on the gun practically remains constant; at a vacuum of approximately 0.05 mm Hg (14 and 15 divisions of the scale), small changes in voltage (for example, by 3 kv) lead to a sharp increase in the working current from 250 to 450 microamps.

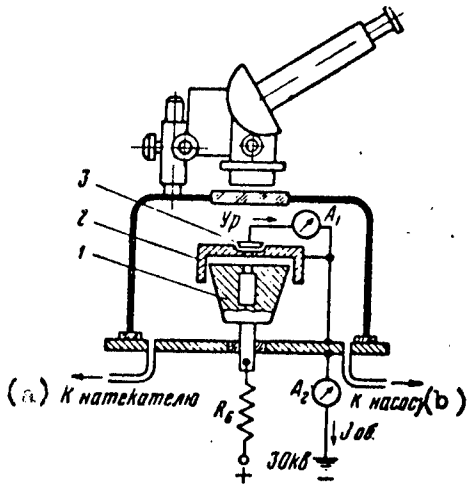

Figure 2
Plan of ion gun. a) to accumulator; b) to pump.

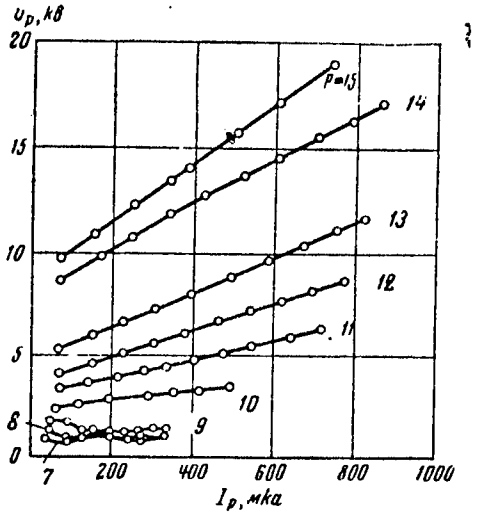

Figure 3
Volt-ampere characteristic. (pressure shown in divisions of middle scale of VT-2 vacuumeter).

One and the same working current may be produced at various pressures in the chamber, but at low vacuum, the voltage on the gun is slight and the total power of the ion gun is low. This condition of operation is not advisable from the technological point of view. With an increase in the vacuum, the accelerating voltage increases and, consequently, the kinetic energy of the ions increases, which, undoubtably, increases the intensity of removal of material from the part. This regularity is more fully shown on figure 4. It can be seen from the graphs that the are of pressures from divisions 7 to 10 are clearly unsuitable, since the total power of the ion gun will not exceed 2 watts. At the same time, at a higher vacuum, equal to 0.05 mm Hg, the power of the ion beam is increased to 10--13 watts, which significantly accelerates the process of treatment.

Working in the pressure range 0.5--0.05 mm Hg as suitable also because the share of working current in the total current increases with an increase in the vacuum. As is shown in fig 5, at pressures near

0.5 mm Hg, 30% of the total current is used for treatment of the part. This is explained by the insufficient focusing of the ion beam, since the resistance of the discharge gap is low and, consequently, the tension of the electrical field between the electrodes of the gun is also low. With increasing vacuum, the resistance of the discharge gap is sharply increased, field intensity increases, and focusing of the gun is improved. At pressures near 0.05 mm Hg (divisions 13 and 15), the working current is 75--85% of the total current.

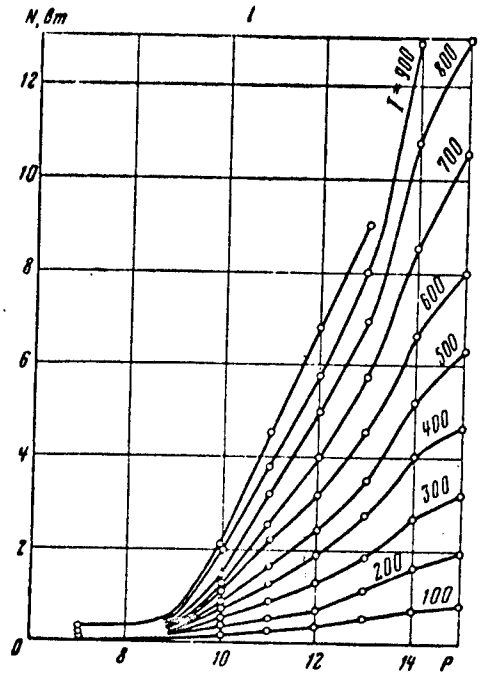

Figure 4
Dependence of ion beam power on chamber pressure

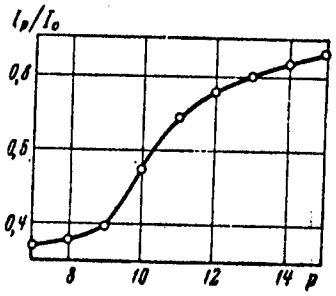

Figure 5
Change in $\frac{I_w}{It}$ with increasing vacuum

The volt-ampere characteristics are also used to define the range of existence of the discharge used for material processing. At pressures near atmospheric, the discharge occurs at voltages nearly coinciding with the potential for ionization of the given gasses. But due to the fact that the field strength is very slight, the ion beam is

poorly focused, the kinetic energy of the ions is slight, and processing is impossible. Increasing the current in this case leads only to intense heating of the part in the area of ion bombardment. Therefore the ion boundary of the vacuum can be considered as 0.5 mm Hg.

At pressures less than 0.05 mm Hg, the discharge is unstable, since the number of gas molecules is insufficient to support a stable gas discharge. With further increase of the vacuum (near 0.02 mm Hg), the discharge no longer occurs even at gun voltages of 30 kv. In connection with this, it can be stated approximately that the working range of the gun is 0.5--0.05 mm Hg.

Technological Characteristics of Method 5

The intensity of the removal of metal depends on the kinetic energy of the ions and the magnitude of the ion current. It is obvious that increases in voltage and current accelerate the process of hole production, but great increases in the voltage cause the appearance of hard X-rays, and increases in the ion current hinder focusing of the beam. Therefore in practice, the voltage to the gun should not exceed 15 kv, and the current should not exceed 1000 microamperes. The magnitude of the ion current depends on the pressure within the chamber (0.05 0.05 mm Hg), so that by regulating the gas feed from the accumulator it isspossible to regulate the ion current from 50 to 1000 microamps. Currents from 50 to 200 the "soft" condition range, are used for penetration of material of small thickness (0.5 mm), when holes of 5--8 microns diameter must be produced. The penetration of thicker material (up to 0.5 mm /sic/) requires greater current to speed up the process.

Approximate conditions and time necessary for treatment of various materials are shown in the table.

The accuracy and cleanliness of the surface of the holes produced depends on the electrical conditions, on the structure of the initial material, on the accuracy of manufacture and assembly of the ion gun, on the pressure of the gas within the chamber and on a number of other factors. If the process takes place at a pressure on the order of 0.5 mm Hg, oxidation of the surface of active materials is possible. When the pressure was decreased to 0.05 mm Hg, oxidation was not observed. In order to eliminate oxidation when working in any operating conditions, the chamber must be filled with a neutral gas (Ar, Cl) and fed during the treatment process.

The structure of the initial material also influences the accuracy of the holes obtained. With large-grain material structure, the material is more actively destroyed at the grain boundaries, and the hole can be made off-round, with projecting edges. When small-grained material is processed, as a rule, round holes are formed.

The diameter of the holes is controlled visually directly during the treatment process with the help of a binocular microscope. The initial diameter of the hole is on the order of 3 microns. Further bombardment causes the diameter to increase to the required size, the diameter being controllable to an accuracy of 1--2 microns.

Table

(a) Материал	(b) Толщина детали, мм	(c) Диаметр отверстия, мк	(d) Напряжение, кв	(e) Ток, мка	(f) Время, мин
(g) Медь МІ, МБ	0,5	65	13	600	15
(h) Нихром	0,03	30	7—10,3	400—200	3
(i) Вольфрам	0,03	10	5,6	100	12
(j) Титан	0,1	50	16	800	60
(k) Германий	0,45	50	8,7	300	12—14
(l) Керамика стеатит	0,28	25	6,3—7	150—200	25
(m) Стекло	0,45	30	7—8,7	200—300	90
(n) Ст. IX18H9T	0,33	30	10,5	400	—

Key: a) material; b) part thickness, mm; c) hole diameter, microns; d) voltage, kv; e) current, microamperes; f) time, minutes; g) copper MI, MB; h) nichrome; i) tungsten; j) titanium; K) germanium; l) steatite ceramic; m) glass; n) 1Kh18N9T steel. Note: pressure in the working chamber was $2 \cdot 10^{-1}$ mm Hg.

As can be seen from the table, the times and working conditions for various materials are different. Such materials as Cu, W, Mo, Ge nichrome and Ta are easily broken down by the action of the ion bombardment. Such materials as titanium, stainless steel, glass and silicon are much harder to process. In processing glass, ceramics and other nonconducting materials, it must be kept in mind that the presence of the dielectric distorts the electric field on the cathode portion of the gun, and the ion beam is partially defocused. In order to improve the focus, it is recommended that one side of the part be covered with a thin film of gallium or a mixture of gallium and indium. The thin conducting layer restores the electric field, and allows perforation of the same small holes in dielectrics as in metals.

Preliminary results obtained in tests of the ion method of producing holes allow the following conclusions to be made.

A well focused ion beam can be successfully used for measured treatment of metals.

In creation of an industrial apparatus for the ion perforation of materials, it will be necessary first of all to increase productivity and assure automatic control of the hole diameter.

The ion perforation method assures vacuum cleanliness of the treated part and requires no subsequent chemical processing as is needed with electrical discharge perforation.

A great advantage of the ion method is its ability to be used for processing of both metals and non-metallic materials.

The main deficiency of the method is its small productivity and the great conicity of the holes produced.

BIBLIOGRAPHY

1. B. R. Lazarenko and N. I. Lazarenko, Elektroiskrovaya Obrabotka Tokoprovodyashchikh Materialov /Electrical Discharge Treatment of Conducting Materials/, Moscow, Academy of Sciences Publishing House, 1958.

2. N. V. Rabotzey and A. Ya. Yukhvidin, USSR Author's Certificate No. 107754, class 491, 12, 1956.

3. L. B. Rezenfeld and A. I. Markov, Byulleten Izobreteniy /Bulletin of inventions/ No 11, 1959, USSR Authors' Certificate No. 120403, class 491, 12.

4. N. A. Kantsov, Elektricheskie Yavleniya v Gazakh i Vakuume /Electrical Phenomena in Gasses and Vacuum/, Moscow, State Technical Publishing House, 1947.

5. V. K. Popov, A. Kh. Balman and M. N. Kalinychev, "The production of very small holes with an ion beam," Voprosy Radioelectroniki /Questions of electronics/ series 1, issue 11, 1961.

6508
CSO: 1879-D/PE

- END -